APL Photonics

Non-resonant recirculating light phase modulator

Cite as: APL Photonics **7**, 106102 (2022); https://doi.org/10.1063/5.0103558
Submitted: 16 June 2022 • Accepted: 09 September 2022 • Accepted Manuscript Online: 09 September 2022 • Published Online: 04 October 2022

Haijin Huang, Xu Han, Armandas Balčytis, et al.

Non-resonant recirculating light phase modulator

Cite as: APL Photon. 7, 106102 (2022); doi: 10.1063/5.0103558
Submitted: 16 June 2022 • Accepted: 9 September 2022 •
Published Online: 4 October 2022

Haijin Huang,[1] Xu Han, Armandas Balčytis,[1] Aditya Dubey,[1] Andreas Boes,[1,3,4] Thach G. Nguyen,[1] Guanghui Ren,[1] Mengxi Tan,[1] Yonghui Tian,[2] and Arnan Mitchell[1,a)]

AFFILIATIONS

[1] Integrated Photonics and Applications Centre, School of Engineering, RMIT University, Melbourne, VIC 3001, Australia
[2] Key Laboratory for Magnetism and Magnetic Materials of MOE, School of Physical Science and Technology, Lanzhou University, Lanzhou 730000, Gansu, China
[3] School of Electrical and Electronic Engineering, The University of Adelaide, Adelaide, SA 5005, Australia
[4] Institute for Photonics and Advanced Sensing, The University of Adelaide, Adelaide, SA 5005, Australia

[a)] **Author to whom correspondence should be addressed:** arnan.mitchell@rmit.edu.au

ABSTRACT

High efficiency and a compact footprint are desired properties for electro-optic modulators. In this paper, we propose, theoretically investigate, and experimentally demonstrate a recirculating phase modulator, which increases the modulation efficiency by modulating the optical field several times in a non-resonant waveguide structure. The "recycling" of light is achieved by looping the optical path that exits the phase modulator back and coupling it to a higher order waveguide mode, which then repeats its passage through the phase modulator. By looping the light back twice, we were able to demonstrate a recirculating phase modulator that requires nine times lower power to generate the same modulation index of a single pass phase modulator. This approach to modulation efficiency enhancement is promising for the design of advanced tunable electro-optical frequency comb generators and other electro-optical devices with defined operational frequency bandwidths.

I. INTRODUCTION

Optical modulators are a vital component in communication systems[1] and microwave photonic devices[2–5] as they provide the means to translate high speed electrical signals into the optical domain, where they can be further processed or propagate over kilometer length scales in optical fibers while experiencing minimal losses. Modulators can also be used for achieving desired on-chip functionalities, such as non-reciprocal devices.[6] While many optical modulators have been demonstrated using materials, such as silicon,[5] indium phosphide,[7] 2D materials,[8] and polymers,[9] arguably one of the most attractive platforms used for electro-optical functionalities is lithium niobate, owing to its low optical losses and high-speed modulation capacity.[1]

Lithium niobate modulators have been commercially available for several decades and have been crucial in the success of optical fiber communications that underpin the Internet.[1] Traditional lithium niobate devices use titanium indiffused waveguides, however, a new generation of thin film silicon and indium phosphide integrated photonics has emerged offering improved drive voltage, compactness, and the potential for system integration.[1] More recently, a similar revolution has taken place in the field of lithium niobate photonics with the emergence of the thin-film lithium niobate waveguide platform offering high efficiencies for electro-optic interaction, and nonlinear optical processes due to the strong modal confinement.[10–12] Nevertheless, there are design choices that need to be considered for efficient modulators in this platform such as the trade-off between the length and bandwidth of modulators[13] or the trade-off for the closeness of the electrode to the waveguide[14] and microwave losses of the electrodes.[12] Optical structures have also been investigated to improve modulation efficiency. For example, loop mirrors[15] and Fabry–Perot cavities[16] have been demonstrated to increase the electro-optical interaction length. Recently, a promising way to increase the interaction length between a waveguide and a thermal heating element was demonstrated, providing an enhanced efficiency for tuning the phase of light by "recycling" or recirculating it several times through the same multimode waveguide, achieved by looping the light back and coupling it to the multimode waveguide using mode multiplexers.[17]

In this article, we investigate if a conceptually similar light recirculation approach can be used for high-speed electro-optical modulators, and how this concept can help to increase the efficiency

of phase modulators. We experimentally demonstrate that the recirculating phase modulator increases the modulation efficiency with the number of recirculations. This enabled us to reduce the power of the microwave signal by a factor of 9 when the light passed three times through the phase modulator when compared with a standard single pass phase modulator with the same electrode dimensions to achieve the same modulation depth.

II. DEVICE CONCEPT

The efficiency of an electro-optic device is directly related to the interaction length between the electrode and the electro-optic waveguide. One option is to make this interaction region as long as possible. We explore an alternative where light is recirculated several times through a phase modulator to improve the modulation efficiency. This is fulfilled by looping the light through different orthogonal modes in a multimode waveguide and applying microwave modulation simultaneously to all the different copropagating modes. Figure 1(a) illustrates the proposed recirculating modulator with two light recycling loops that are described as a case-in-point in detail as follows.

In the proposed recirculating modulator, the light is coupled into a single mode waveguide in the form of the TE0 mode on the left side. It passes through two tapers that increase the waveguide width, making it a multimode such that it supports TE0 and TE1 modes after the first taper and TE0, TE1, and TE2 modes after the second taper. The optical field intensity plots of modes supported in the waveguide after the second taper are illustrated in Fig. 1(d). After passing through the two tapers, the input optical power remains predominantly in the TE0 mode, which gets modulated by the microwave signal applied to the traveling wave electrodes, similar to a conventional phase modulator. A schematic cross-section of a modulator in the SiN loaded thin-film lithium niobate on the insulator platform is shown in Fig. 1(c). Afterward, the multimode waveguide is tapered down in two stages back to the width of a single mode waveguide, which is then looped back to the input side, where it is coupled as the TE1 mode to the multimode waveguide, using mode multiplexers described in our previous work.[18] The TE1 mode passes again through the same traveling wave electrodes, experiencing a second modulation. Subsequently, the TE1 mode is coupled to a single TE0 mode waveguide using a mode multiplexer. The single mode waveguide is looped back again, where it is coupled as a TE2 mode to the multimode waveguide. The TE2 mode is then modulated again before it is coupled out as a TE0 mode to a single mode output waveguide. FDTD simulated operation of the TE0-TE1 and TE0-TE2 mode converters is shown in Fig. 1(b).[18] In principle, the number of loops can be increased arbitrarily, but it comes at a cost of device footprint and might require wider electrode gaps, as the width of the multimode waveguides needs to increase to accommodate the additional higher order modes.

III. THEORETICAL ANALYSIS

In this section, we have a closer look at the recirculating modulator operation and what considerations need to be taken into account to achieve an increased modulation efficiency. When a sinusoidal signal $V(t) = A\sin(\omega_s t)$ is applied to a single pass phase modulator, the output optical field from the device can be expressed as

$$E_{out} = E_o e^{i\omega_c t} e^{iR\sin\omega_s t} = E_o e^{i\omega_c t}\sum_{n=-\infty}^{n=+\infty} J_n(R) e^{in\omega_s t}, \quad (1)$$

where E_o and ω_c are the amplitude and angular frequency of the optical carrier, ω_s is the angular frequency of the radio frequency (RF) modulating signal, R is the modulation index, which is equal to $\pi A/V_\pi$, where A is the amplitude of microwave signal and V_π is the voltage required to shift the phase of the carrier by π, and J_n is the Bessel function of the first kind. In the case of a recirculating

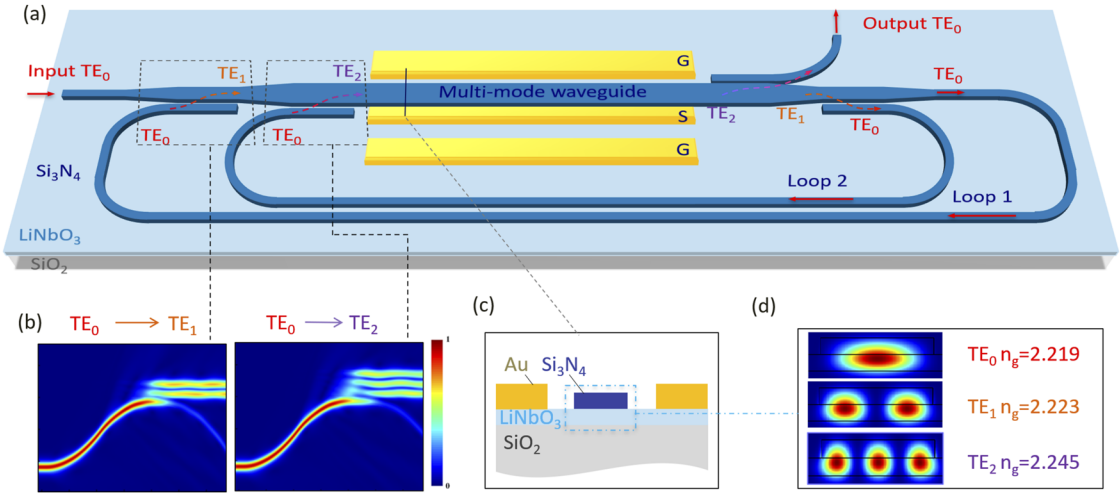

FIG. 1. (a) Schematic of a recirculating phase modulator, (b) simulated mode multiplexer for coupling the TE0 to TE1 mode and coupling the TE0 to TE2 mode, (c) cross section of the multimode phase modulator electrode region, and (d) normalized optical field plots for the TE0, TE1, and TE2 modes.

modulator, as introduced in Fig. 1(a), the light is modulated multiple times, which for N recirculations can be expressed as

$$E_{out} = E_o e^{i\omega_c t} e^{iR_0 \sin\omega_s t} e^{iR_1 \sin\omega_s (t-\Delta T_1)} \times e^{iR_2 \sin\omega_s (t-\Delta T_2)} \ldots e^{iR_N \sin\omega_s (t-\Delta T_N)}, \quad (2)$$

where R_j ($j = 0, 1, 2, \ldots, N$) is the modulation index of the jth recirculation and ΔT_j ($j = 1, 2, \ldots, N$) is the loop transit time for light to re-enter the modulator, which is effectively the time delay between two different modes be modulated by the RF electrode. The loop transit time is given by $\Delta T_j = \Delta L_j / v_g$, where ΔL_j is the length of loop j and v_g is the group velocity of the fundamental mode TE_0 in the loop waveguides. If one assumes that the modulation index is the same for all modes, Eq. (2) can be written as

$$E_{out} = E_o e^{i\omega_c t} e^{iR * \kappa * \sin(\omega_s t - \varphi)}, \quad (3)$$

where $\varphi = \arctan \frac{\sin\omega_s\Delta T_1 + \sin\omega_s\Delta T_2 + \cdots + \sin\omega_s\Delta T_n}{1 + \cos\omega_s\Delta T_1 + \cos\omega_s\Delta T_2 + \cdots + \cos\omega_s\Delta T_n}$ and the κ is the enhancement factor of the recirculating modulator. In the case of Nth recirculation, the enhancement factor can be expressed as

$$\kappa = \sqrt{(1 + \cos\omega_s\Delta T_1 + \cos\omega_s\Delta T_2 + \cdots + \cos\omega_s\Delta T_N)^2 + (\sin\omega_s\Delta T_1 + \sin\omega_s\Delta T_2 + \cdots + \sin\omega_s\Delta T_N)^2}. \quad (4)$$

Then, expanding Eq. (3) by Bessel functions of the first kind, the output signal can be described as

$$E_{out} = E_o e^{i\omega_c t} * \sum_{n=-\infty}^{n=+\infty} J_n(R * \kappa) * e^{in(\omega_s t - \varphi)}. \quad (5)$$

As one can see from Eqs. (4) and (5), the output signal is strongly dependent on the enhancement factor, which is determined by modulation frequency ω_s and the delay time ΔT_j for each recirculating loop. Maximum enhancement factor can be achieved when $\Delta T_j = 2m\pi/\omega_s$, where m is an integer. For N recirculations, the maximum enhancement factor is equal to $N + 1$.

IV. DEVICE DESIGN

For investigating the recirculating modulator, we chose the SiN loaded thin-film lithium niobate on the insulator platform, see Fig. 1(a) and our pervious works,[18,19] with a 0.3 μm thick lithium niobate film and a 0.3 μm thick silicon nitride thickness. The waveguide widths needed to support the three different waveguide modes were 1.2, 2.8, and 4.5 μm in accordance with the mode multiplexers in Ref. 18. For the traveling wave electrode, we chose an electrode separation of 9.5 μm and a gold metal thickness of 0.5 μm. The $V_\pi L$ of the TE0, TE1, and TE2 modes was calculated to be 7.38, 7.35, and 7.52 Vcm.

In designing prototype recirculating phase modulators, we chose a 25 GHz operation frequency. The group indices of the TE0, TE1, and TE2 mode for a waveguide width of 1.2, 2.8, and 4.5 μm are 2.233, 2.241, and 2.245, respectively. When considering the group index of the TE_0 in loop waveguides $n_g = 2.233$, calculations show that for the device to operate at its highest enhancement factor the waveguide lengths for TE0 and TE1 loops have to, respectively, be 21.5 mm and 16.1 mm, which corresponds to an m of 4 and 3, respectively. To confirm this, we simulated the enhancement factor as a function of the modulation frequency, which is shown in Fig. 2. One can see that the conventional single-pass phase modulator has an enhancement factor of 1 for all frequencies (assuming ideal operation). Conversely, a single loop recirculating modulator has a periodic response, reaching an enhancement factor of $\kappa \sim 2$ at 0, 6.3, 12.5, 18.8, 25, 31.3, and 37.5 GHz, while the dual loop recirculating modulator reaches an enhancement factor of $\kappa \sim 3$ for 0 and 25 GHz. This shows that we should expect an increase of the enhancement factor to 3 when looping the light back twice and operating at 25 GHz with delay lengths of 21.5 mm and 16.1 mm for the two loops. As the group indices of the three modes are all within 0.6%, they have negligible influence on the device performance when compared with the large RF wavelengths that they need to be phase matched to.

V. EXPERIMENTAL RESULTS

To prove the device performance, we fabricated the designed 25 GHz operation frequency recirculating modulator devices with one and two loops and benchmarked them against a traditional single-pass phase modulator. Fabrication was performed following

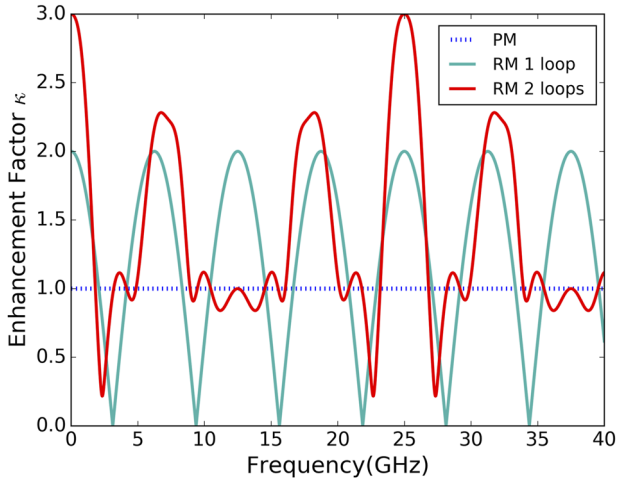

FIG. 2. Enhancement factors as a function of the modulation frequency for single and a dual loop recirculating phase modulators A typical single-pass phase modulator exhibits a frequency independent baseline $\kappa = 1$ enhancement factor.

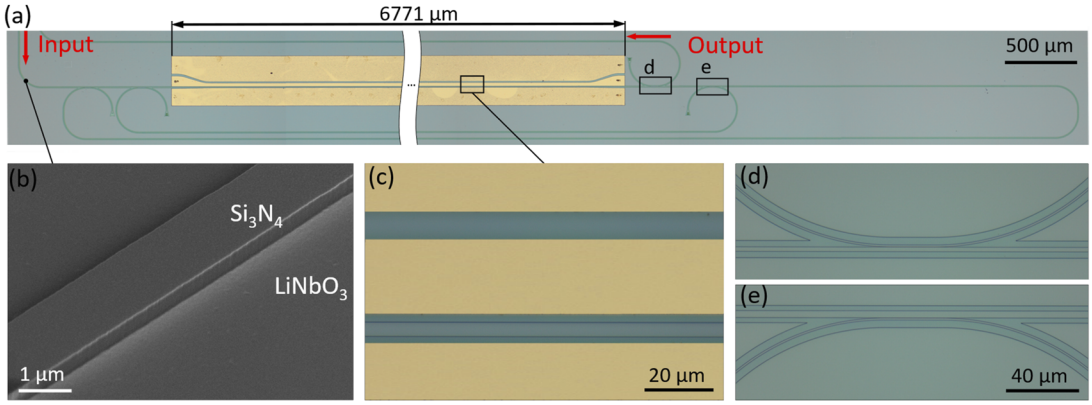

FIG. 3. (a) Optical microscope image of recirculating phase modulator device with two loops, (b) scanning electron micrograph of a fabricated single mode waveguide, (c) traveling wave electrode alignment to the multimode waveguide, (d) fabricated mode multiplexer to couple the TE2 to a TE0 mode, and (e) mode multiplexer for coupling the TE1 mode to a TE0 mode.

the steps outlined in our prior work.[18] In brief, optical waveguiding in thin-film lithium niobate [see Fig. 3(b)] is established by depositing a SiN loading layer by means of reactive sputtering,[20] followed by patterning this SiN film using electron beam lithography and reactive ion etching. Gold electrodes [Fig. 3(c)] comprising the electro-optical modulator section were formed using laser lithography patterning with a subsequent physical vapor deposition and lift-off process. The fabricated device with two recirculation loops is shown in Fig. 3(a). The on-chip footprint of this device is 10.85 × 0.66 mm^2, and the active modulation section takes up 62% of the total device length.

To characterize the performance of the recirculating modulators, we couple 1550 nm light into the devices and applied an amplified 25 GHz microwave signal from an Anritsu MG3694A frequency synthesizer to the traveling wave electrodes and measured the resulting spectra with a Finisar WaveAnalyzer 1500S High-Resolution Optical Spectrum Analyzer. The output of the electrodes was terminated with 50 Ω impedance matching terminators. Figures 4(a)–4(c) show the measured spectra when a 25 dBm RF power is applied to a typical single-pass phase modulator as well as recirculating phase modulators with one and two loops, respectively. These modulators have the same electrode length, gap, and thickness. One can see that the overall optical power levels for the graphs are slightly different, which is most likely caused by fabrication errors as well as increased losses for the recirculating modulators with two loops, due to the increased waveguide length and additional mode multiplexing structures. One can also see that a recirculating modulator can generate more sidebands compared with a conventional phase modulator. To estimate the modulation index, we fitted the power of sideband power using Eq. (1) and found that the modulation index approximately doubled for the single loop recirculating modulator and tripled for the two loops recirculating modulator [see black dots in Figs. 4(a)–4(c)], when compared with a single-pass phase modulator. These results matched well with our prediction of how the enhancement factor scales with the number of loops, as shown in Fig. 2.

Next, we characterized the modulation efficiency of the different modulators by adjusting the applied RF power so that the spectra exhibit the same modulation index (same power distribution of the sidebands) as compared with the single-pass phase modulator. The

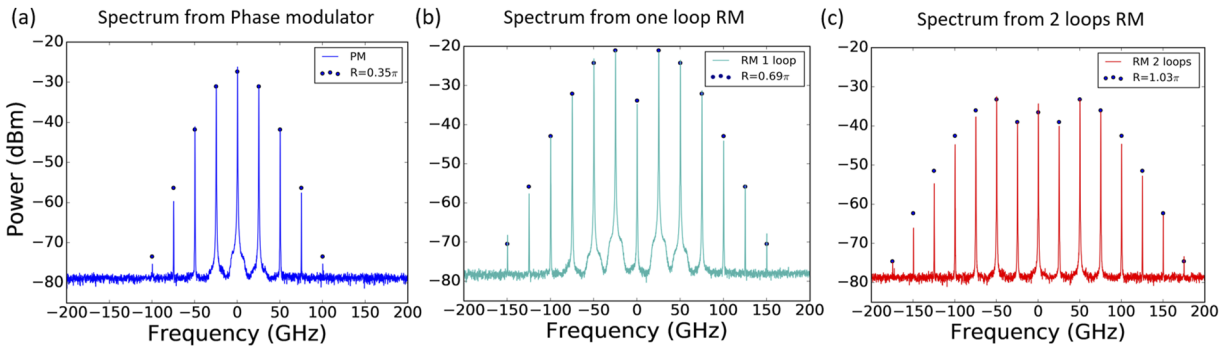

FIG. 4. Measured spectra for (a) single mode phase modulator, (b) single loop, and (c) two loop recirculating modulators when 25dBm RF power is applied.

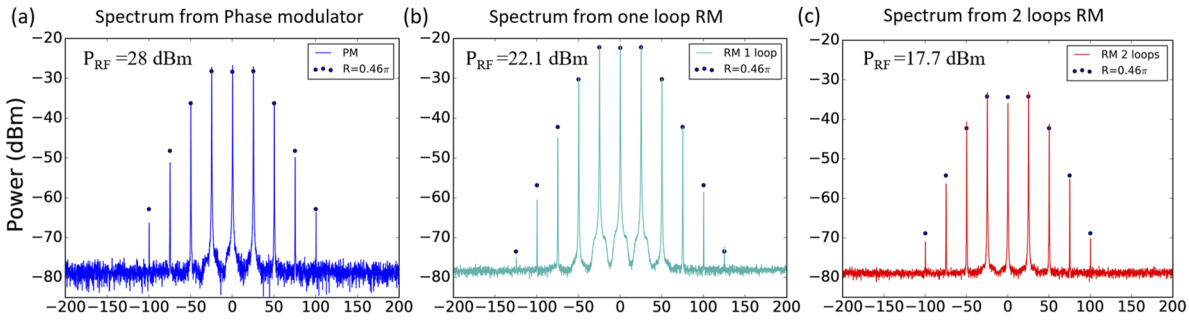

FIG. 5. Equivalent spectra generated by (a) single mode phase modulator (28 dBm RF power), (b) one loop (22.1 dBm RF power), and (c) two loop recirculating phase modulators (17.7 dBm RF power).

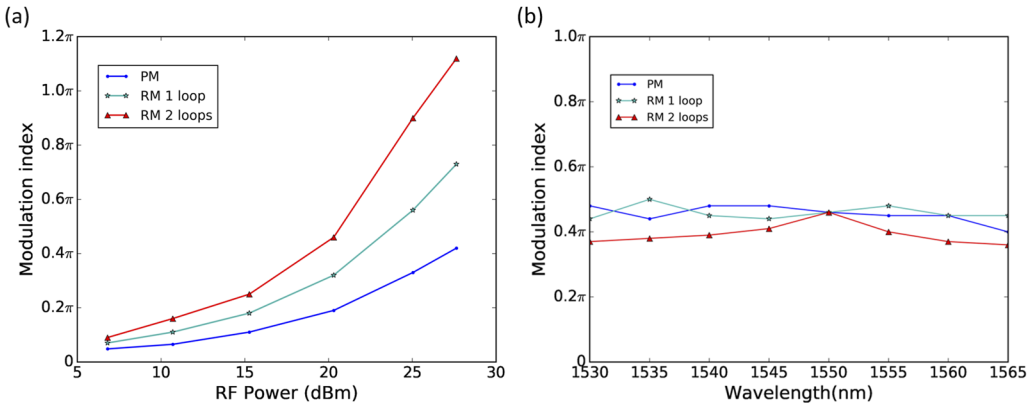

FIG. 6. (a) Modulation index of a conventional phase modulator and the recirculating modulators with one and two loops as a function of the applied RF power. (b) The modulation index of the different modulators as a function of the operation wavelength in the C-band.

results are shown in Figs. 5(a)–5(c), which show that the single-pass phase modulator, as well as the single loop and dual loop recirculating phase modulators, exhibit the same modulation index, while the applied microwave power decreases from 28 to 22.1 and 17.7 dBm, respectively. This corresponds well to the theoretical prediction of the RF power reduction for a single loop recirculation, which is 2^2 (6 dB), and for a dual loop, recirculation is 3^2 (9.5 dB). This indicates that the dual loop recirculating phase modulator requires approximately one order of magnitude less RF power to achieve the same modulation index, increasing the modulation efficiency significantly.

To analyze the modulation efficiency, we measured the modulation index of the modulators for different RF powers. The results are presented in Fig. 6(a). One can see that the modulation index has a near quadratic dependence on the RF power, which matches the RF power scaling with applied voltage. One can also observe how the modulation index for the recirculating modulators increases by a factor of ~2 for a single loop recirculating modulator and ~3 for a dual loop recirculating modulator compared with the single pass phase modulator with an equivalent electrode configuration. This demonstrates that light recirculation in modulators can notably improve their modulation efficiency.

Since recirculating phase modulators are optically not resonant, one would expect that the spectral bandwidth of the modulators is broad and mainly limited by the wavelength dependence of the mode multiplexers. To characterize the optical bandwidth, we applied the RF power for which the modulator operates with a modulation index of 0.46π and recorded the modulation index as a function of wavelength from 1530 to 1565 nm, in steps of 5 nm. The results are presented in Fig. 6(b), which shows that the modulation index is not notably influenced by the operation wavelength. The observed small fluctuations of the modulation index may be caused by the wavelength dependency of the mode multiplexers.

VI. DISCUSSION

Experimental demonstration of the recirculating modulator has shown that increasing the number of loops does indeed increase the modulation efficiency. Although this is highly attractive, one also needs to consider the trade-offs that come with such a design. For example, one should be aware that the operation bandwidth of the modulator is decreased and that adding more loops to the recirculating phase modulators may result in higher optical losses.

There is also a practical limitation on the loop number scalability, as higher order multimode waveguides will be required, causing the waveguide modes to be closer in their effective indices, which can lead to enhanced cross talk between the modes. Furthermore, a wider multimode waveguide will increase the separation of electrodes, resulting in a higher V_π of modulators. In our experimental demonstration, we chose an electrode gap of 9.5 μm, which was chosen as a conservative value to ensure that the optical modes in the multimode waveguide do not suffer from optical losses due to interaction with the electrodes, which includes considerations about the alignment tolerances for the fabrication of the electrodes. Smaller electrode gaps are feasible, which can help to increase the modulation efficiency of the recirculating modulator.

Another point to note is that the current design of the recirculating modulator only uses one gap of the traveling wave modulator for modulation (the second gap is not used) and that the light that is routed back for recirculation is not modulated on the return path. Both points present opportunities to increase the modulation strength of the recirculating modulator, without increasing the device footprint. For example, one could consider adding a second traveling wave electrode on the waveguide path that brings the light back for recirculation. However, this addition would come at the expense of a second RF signal that needs to be applied to the electrodes, which may not be desirable. Alternatively, one can consider RF electrodes with a "U" bend so that they modulate the light in the waveguide that is looped back.[21] This would remove the requirement for an additional RF signal, but the RF losses in extended electrodes may result in weaker modulation. Another opportunity to increase the modulation strength is to use the second gap of the traveling wave modulator electrode; however, the RF wave would be counter-propagating to the optical wave, which may result in a weaker modulation. Using lump electrodes instead of traveling wave electrodes can help ensure that the modulation strength for light in both directions is equal.

These opportunities to increase the modulation strength and efficiency of the investigated recirculating phase modulators further are highly attractive for applications for the generation of electro-optical frequency combs,[22,23] where one can apply a known and constant RF signal. The advantage of the recirculating modulator is that RF losses of the electrodes are less of a concern compared with high efficiency modulators that rely on long electrodes. It may also become possible to consider such devices for optical computational tasks, as the looping back through the same modulator offers the imprinting of different electrical signals in time onto the optical domain Ref. 24.

VII. CONCLUSION

In this work, we present a new recirculating phase modulator concept, explore its properties through numerical simulations, and experimentally validate the performance of a prototype device fabricated on the thin-film lithium niobate on the insulator platform. The recirculating modulators with two light recycling loops exhibit an approximately threefold increase in modulation efficiency, enabling a reduction of the microwave power required for achieving the same modulation index by approximately one order of magnitude. We also provide the numerical expression of the enhancement factor for Nth recirculation case, which provides the possibility for further improvement in the future. Moreover, we believe such modulators pave the way to reduce the power required for electro-optical frequency comb generation and for executing optical computation tasks.

ACKNOWLEDGMENTS

This work was supported by the Australian Research Council (ARC) under Award No. ARC DP190102773.

AUTHOR DECLARATIONS

Conflict of Interest

The authors have no conflicts to disclose.

Author Contributions

Haijin Huang: Conceptualization (equal); Data curation (equal); Writing – original draft (equal). **Xu Han**: Investigation (supporting). **Armandas Balčytis**: Investigation (supporting); Supervision (supporting); Writing – review & editing (supporting). **Aditya Dubey**: Investigation (supporting). **Andreas Boes**: Investigation (supporting); Supervision (supporting); Writing – review & editing (supporting). **Thach G. Nguyen**: Investigation (supporting); Supervision (supporting); Writing – review & editing (supporting). **Guanghui Ren**: Investigation (supporting); Supervision (supporting); Writing – review & editing (supporting). **Mengxi Tan**: Investigation (supporting); Writing – review & editing (supporting). **Yonghui Tian**: Investigation (supporting). **Arnan Mitchell**: Investigation (equal); Supervision (equal); Writing – review & editing (equal).

DATA AVAILABILITY

The data that support the findings of this study are available from the corresponding author upon reasonable request.

REFERENCES

[1] E. L. Wooten *et al.*, "A review of lithium niobate modulators for fiber-optic communications systems," IEEE J. Sel. Top. Quantum Electron. **6**(1), 69–82 (2000).
[2] D. Marpaung, J. Yao, and J. Capmany, "Integrated microwave photonics," Nat. Photonics **13**(2), 80–90 (2019).
[3] P. Ghelfi *et al.*, "A fully photonics-based coherent radar system," Nature **507**(7492), 341–345 (2014).
[4] T. M. Fortier *et al.*, "Generation of ultrastable microwaves via optical frequency division," Nat. Photonics **5**(7), 425–429 (2011).
[5] G. T. Reed, G. Mashanovich, F. Y. Gardes, and D. J. Thomson, "Silicon optical modulators," Nat. Photonics **4**(8), 518–526 (2010).
[6] L. D. Tzuang, K. Fang, P. Nussenzveig, S. Fan, and M. Lipson, "Non-reciprocal phase shift induced by an effective magnetic flux for light," Nat. Photonics **8**(9), 701–705 (2014).
[7] Y. Ogiso *et al.*, "Over 67 GHz bandwidth and 1.5 V Vπ InP-based optical IQ modulator with n-i-p-n heterostructure," J. Lightwave Technol. **35**(8), 1450–1455 (2017).
[8] S. Yu, X. Wu, Y. Wang, X. Guo, and L. Tong, "2D materials for optical modulation: Challenges and opportunities," Adv. Mater. **29**(14), 1606128 (2017).

[9]M. Lee *et al.*, "Broadband modulation of light by using an electro-optic polymer," Science **298**(5597), 1401–1403 (2002).
[10]G. Poberaj, H. Hu, W. Sohler, and P. Günter, "Lithium niobate on insulator (LNOI) for micro-photonic devices," Laser Photonics Rev. **6**(4), 488–503 (2012).
[11]A. Boes, B. Corcoran, L. Chang, J. Bowers, and A. Mitchell, "Status and potential of lithium niobate on insulator (LNOI) for photonic integrated circuits," Laser Photonics Rev. **12**(4), 1700256 (2018).
[12]M. Zhang, C. Wang, P. Kharel, D. Zhu, and M. Lončar, "Integrated lithium niobate electro-optic modulators: When performance meets scalability," Optica **8**(5), 652–667 (2021).
[13]A. N. R. Ahmed, S. Nelan, S. Shi, P. Yao, A. Mercante, and D. W. Prather, "Subvolt electro-optical modulator on thin-film lithium niobate and silicon nitride hybrid platform," Opt. Lett. **45**(5), 1112–1115 (2020).
[14]M. Jin, J. Chen, Y. Sua, P. Kumar, and Y. Huang, "Efficient electro-optical modulation on thin-film lithium niobate," Opt. Lett. **46**(8), 1884–1887 (2021).
[15]J. Jian *et al.*, "High modulation efficiency lithium niobate Michelson interferometer modulator," Opt. Express **27**(13), 18731–18739 (2019).
[16]B. Pan *et al.*, "Compact electro-optic modulator on lithium niobate," Photonics Res. **10**(3), 697–702 (2022).
[17]Y.-C. Chang, S. P. Roberts, B. Stern, and M. Lipson, "Resonance-free light recycling," arXiv:1710.02891 (2017).
[18]X. Han *et al.*, "Mode and polarization-division multiplexing based on silicon nitride loaded lithium niobate on insulator platform," Laser Photonics Rev. **16**(1), 2100529 (2022).
[19]P. Zhang *et al.*, "High-speed electro-optic modulator based on silicon nitride loaded lithium niobate on an insulator platform," Opt. Lett. **46**(23), 5986–5989 (2021).
[20]A. Frigg *et al.*, "Low loss CMOS-compatible silicon nitride photonics utilizing reactive sputtered thin films," Opt. Express **27**(26), 37795–37805 (2019).
[21]S. Sun *et al.*, "Folded heterogeneous silicon and lithium niobate Mach–Zehnder modulators with low drive voltage," Micromachines **12**(7), 823 (2021).
[22]V. Torres-Company and A. M. Weiner, "Optical frequency comb technology for ultra-broadband radio-frequency photonics," Laser Photonics Rev. **8**(3), 368–393 (2014).
[23]A. J. Metcalf, V. Torres-Company, D. E. Leaird, and A. M. Weiner, "High-power broadly tunable electrooptic frequency comb generator," IEEE J. Sel. Top. Quantum Electron. **19**(6), 231–236 (2013).
[24]C. Qiu, H. Xiao, L. Wang, and Y. Tian, "Recent advances in integrated optical directed logic operations for high performance optical computing: A review," Front. Optoelectron. **15**(1), 1–17 (2022).